Title

Efficient expression, purification, and visualization by cryo-EM of unliganded near full-length HER3.

Authors

Diwanji, Devan
Trenker, Raphael
Jura, Natalia
et al.

Publication Date

2022

DOI

10.1016/bs.mie.2022.03.048

Peer reviewed

HHS Public Access

Author manuscript

Methods Enzymol. Author manuscript; available in PMC 2023 April 05.

Published in final edited form as:

Methods Enzymol. 2022 ; 667: 611–632. doi:10.1016/bs.mie.2022.03.048.

Efficient Expression, Purification, and Visualization by Cryo-EM of Unliganded Near Full-Length HER3

Devan Diwanji[a,b,†], **Raphael Trenker**[a,†], **Natalia Jura**[a,d,*], **Kliment A. Verba**[c,e,*]

[a]Cardiovascular Research Institute, University of California San Francisco, San Francisco, CA 94158, USA

[b]Medical Scientist Training Program, University of California San Francisco, San Francisco, CA 94158, USA

[c]Quantitative Biosciences Institute (QBI), University of California San Francisco, San Francisco, CA 94158, USA

[d]Department of Cellular and Molecular Pharmacology, University of California San Francisco, San Francisco, CA 94158, USA

[e]Department of Pharmaceutical Chemistry, University of California San Francisco, San Francisco, CA 94158, USA

Abstract

Biochemical analyses of membrane receptor kinases have been limited by challenges in obtaining sufficient homogeneous receptor samples for downstream structural and biophysical characterization. Here, we report a suite of methods for the efficient expression, purification, and visualization by cryo-electron microscopy (cryo-EM) of near full-length Human Epidermal Growth Factor Receptor 3 (HER3), a receptor tyrosine pseudokinase, in the unliganded state. Through transient mammalian cell expression, a two-step purification with detergent exchange into lauryl maltose neopentyl glycol (LMNG), and freezing devoid of background detergent micelle, we obtained ~6Å reconstructions of the ~60 kDa fully-glycosylated unliganded extracellular domain of HER3 from just 30 milliliters of suspension culture. The reconstructions reveal previously unappreciated extracellular domain dynamics and glycosylation sites.

1. Introduction: The Human Epidermal Growth Factor Receptor 3 (HER3)

Receptor kinases play critical roles in cell signaling and disease (Du & Lovly, 2018; Lemmon & Schlessinger, 2010). Structural biology and biophysical investigations of receptor kinases in the full-length context are invaluable in probing the fundamental mechanisms by which an extracellular signal may be transmitted across the membrane to modulate the activity of the intracellular kinases (Diwanji et al., 2019). Unfortunately, to date, there are only a handful of structural studies with receptor kinases in their full-length or near full-length forms, all at low resolution (Chen et al., 2015; Gutmann et al., 2018;

*Correspondence should be addressed to N.J. (natalia.jura@ucsf.edu) or K.A.V. (kliment.verba@ucsf.edu).
†Authors contributed equally to the work

Huang et al., 2020; Li et al., 2019; Mi et al., 2008; Mi et al., 2011; Opatowsky et al., 2014; Uchikawa et al., 2019). Major barriers to these structural pursuits are governed by the intrinsic biology of receptor kinases that limit their expression, homogeneous purification, and visualization at high resolutions. Low expression levels, for example, may be attributed to cellular downregulation or cytotoxicity (Goh & Sorkin, 2013). Isolated full-length receptors may exist in numerous oligomeric and/or conformational states or associate with other cellular components yielding an unacceptable level of compositional heterogeneity for structural biology (Diwanji et al., 2019). Even if a homogeneous detergent-solubilized full-length receptor sample is obtained (often from liters of mammalian culture), the sample must be sufficiently concentrated for visualization by single-particle cryo-electron microscopy (cryo-EM) or X-ray crystallography. It is evident that numerous technical bottlenecks have hampered full-length receptor kinase structural biology. Here, we describe the efficient expression, purification, and visualization of near full-length HER3 that may serve as a blueprint for the biophysical investigations of other receptor kinases in their full-length forms.

Receptor tyrosine kinases (RTKs) are single spanning membrane proteins with extracellular domains that bind ligands and intracellular kinases whose catalytic activity regulates downstream signaling. The HER receptor family consists of EGFR, HER2, HER3, and HER4 and is but 1 of 20 RTK families (Lemmon & Schlessinger, 2010). HER3 is a unique member of the HER receptor family as a pseudokinase with divergent residues in the kinase domain that abrogate its catalytic activity (Guy et al., 1994; Jura et al., 2009). Despite evolving into a pseudokinase, HER3 has retained its ability to bind to extracellular ligands such as neuregulin-1β (NRG1β) which triggers HER3 heterodimerization with other catalytically active HER receptors, notably HER2 (Hsieh & Moasser, 2007; Moasser, 2007). HER3 allosterically activates HER2 through the asymmetric kinase domain dimer (Zhang et al., 2006). In the absence of ligand, the HER3 extracellular domain exists in an inhibited conformation that does not permit its association with co-receptors (Cho & Leahy, 2002). The extracellular domains of human HER receptors contain four subdomains: domains I-IV. Domains II and IV form an intramolecular tether in the autoinhibited, “tethered” state. Ligand binding relieves the autoinhibition to promote an extended conformation with dimerization interfaces accessible by co-receptors (Kovacs et al., 2015). In previously solved liganded HER receptor structures, the β-hairpin dimerization arm located in domain II coordinates the dimeric interaction (Ferguson et al., 2003; Kovacs et al., 2015; Lu et al., 2010). This critical dimerization arm remains inaccessible in the unliganded state. Interestingly, unlike all previously solved structures of liganded HER receptors, the HER3 dimerization arm does not engage HER2 owing to the singly-liganded nature of the HER2/HER3 heterodimer (Diwanji et al., 2021).

Heterodimerization enables transphosphorylation of tyrosine residues on the HER3 C-terminal tail (Choi et al., 2020). The HER3 C-terminal tail is remarkable, not only for being the longest tail of the HER family, but also for containing six PI3K consensus binding motifs (YxxM). It is through these phosphorylated YxxM motifs that the HER3 C-terminal tail acts as a “super-scaffold” to potently recruit phosphoinositide-3 kinase (PI3K) to regulate cell survival and proliferation (Hellyer et al., 1998). The PI3K signaling pathway constitutes one of the most frequently deregulated pathways in cancer, rendering HER3 and PI3K as

important therapeutic targets (Kandoth et al., 2013). Structural investigations of HER3 in the inactivated, unliganded state may reveal important regulatory mechanisms that keep HER3-PI3K signaling in check.

Despite our growing knowledge of HER receptor mechanism, our understanding of signal transduction across the membrane is limited without structures containing intracellular and extracellular domains. Numerous questions exist about the unliganded state, especially the organization of the receptor relative to the membrane. For example, how are the unliganded tethered extracellular domains oriented relative to the membrane? Does the membrane mediate potential autoinhibitory interactions with the intracellular juxtamembrane and/or kinase domain? To date, the unliganded state of HER receptors has been characterized by X-ray crystallography with partially deglycosylated extracellular domain samples to facilitate crystallization (Bouyain et al., 2005; Cho & Leahy, 2002). Deglycosylation itself may alter structure. Several studies with HER receptors have shown that the glycosylation state modulates binding to growth factors, dimerization, and recognition by therapeutic agents (Azimzadeh Irani et al., 2017). For example, mutating the HER3 extracellular N-linked glycosylation site, N437, has been shown to promote heterodimerization with HER2 in the absence of ligand (Takahashi et al., 2013; Yokoe et al., 2007). Molecular dynamic simulations provide evidence that EGFR N-linked glycosylation plays a critical role in the binding of growth factors (Azimzadeh Irani et al., 2017). HER2 glycosylation decreases the affinity of the monoclonal antibody Herceptin for HER2 (Peiris et al., 2017). Clearly, structural studies with glycosylated full-length HER receptors can provide invaluable insight into the fundamental mechanism of signal transduction.

Materials and Equipment

125 mL flask non-baffled, vented cap flask, (VWR, #89095-258)

Incubator at 37°C and 8% CO_2 with shaker (Heracell VIOS 160i, Thermo Scientific)

Class II Biosafety Cabinet

Disposable Serological Pipets 5 ml, 10 ml, 25 ml (VWR, #89130)

Conical tubes 15ml, 50 ml (VWR, #21008)

Liquid nitrogen

Table-top microcentrifuge (5424 R, Eppendorf)

Table-top centrifuge (for 15/50 ml conical tubes, Allegra X-15R, Beckman Coulter)

−80°C freezer

Nutating mixer (Fisher scientific)

Micro Bio-Spin columns, 0.8 ml (Bio-Rad, #7326204)

Amicon Ultra-0.5 Centrifugal Filter Units, MWCO 100 kDa (Millipore Sigma, #UFC510096)

Superose6 10/300 Increase (GE Healthcare, now Cytiva, #29-0915-96)

Akta purification system (Akta Pure, Cytiva)

FEI-Tecnai T12

4k CCD camera (Gatan)

GPU-equipped workstation (at least 11GB of GPU memory, at least 128GB of system memory, at least 4TB of fast SSD storage and 20TB of spinning disc storage)

Glow discharger (PELCO easyGlow, Ted Pella)

Formvar/carbon 400 mesh copper grids (Ted Pella, #01754-F)

Quantifoil R1.2/1.3 mesh Au holey-carbon grids Electron Microscopy Sciences, #Q310AR1.3

Vitrobot Mark IV (FEI)

Talos-Arctica 200 kEv (ThermoFisher)

K3 Direct electron detector camera (Gatan)

2. Construct Design and Expression of Near Full-Length HER3

2.1 Near Full-Length Construct Design

We sought to optimize expression and purification of unliganded HER3 to enable reconstitution efforts of the HER2/HER3 heterodimer *in vitro*. We introduced an N-terminal 1x FLAG tag and a C-terminal twin-Strep (TS) tag to the full-length construct of human HER3 in a pFastBac vector (Thermo Fisher Scientific, #10360014) in which a baculovirus promoter was replaced by a CMV promoter for mammalian cell protein expression (Sung et al., 2014). Alternatively, standard pCDNA3 or pCDNA4 vectors may be used for this protocol. As C-terminal tails of HER family receptors are predicted to be unstructured, we chose to express HER3 with most of its C-terminal tail truncated (Δ1022-1342) as the tail could destabilize the receptor or hamper expression. Our near full-length HER3 construct therefore contains the extracellular domain (ECD), the transmembrane domain (TMD), the intracellular kinase domain (KD), and a brief segment of the C-terminal tail retained for kinase stability (Fig. 1A and 1B).

2.2 Efficient Expression in Mammalian Suspension Cultures

Previous structural studies with full-length or near full-length RTKs used adherent or suspension mammalian cell culture for expression (Chen et al., 2015; Gutmann et al., 2018; Huang et al., 2020; Li et al., 2019; Mi et al., 2008; Mi et al., 2011; Uchikawa et al., 2019). We initially expressed our HER3 constructs in adherent format on 15-cm dishes and found that cell material from at least 20 15-cm dishes would be required to be spectroscopically detectable during gel filtration chromatography after purification. Transfection with different lipophilic reagents or titrating plasmid concentrations did not improve expression efficiency. Furthermore, large-scale suspension expression in human embryo kidney (HEK) 293S with BacMAM required culture volumes of more than 6L to net disappointingly low sample yields. Such expression strategies are not cost effective nor time efficient for optimization.

We therefore turned to the Expi293 HEK transient expression system (Life Technologies). In this system, cells cultured to densities of 2–3*10^6 are transfected with a lipophilic transfection reagent and enhanced with two proprietary enhancers 18 hrs post-transfection (Fig. 1C). Our initial expression trials with near full-length HER3 revealed a remarkable boost in expression with maximal expression at 24 hrs post-enhancer. We estimated that 30 mL of culture in the Expi293 system achieved a 100-fold increase in expression compared with 20 15-cm dishes (data not shown). The boost in expression combined with the ease of suspension culture and short incubation times allowed us to parallelize optimization at a small scale which would have simply not been feasible with previous expression strategies.

3. Purification and Initial Visualization of Homogeneous Near Full-Length HER3 Sample

3.1 Streamlined Purification of Near Full-Length HER3

Purification of unliganded near full-length HER3 begins with detergent extraction from flash-frozen cell pellets from 30 mL of suspension culture. Our lysis buffer contains ethylenediaminetetraacetic acid (EDTA) to chelate residual Mg^{2+} and $NaVO_3$ to inhibit phosphatases. We reasoned that kinase inactivation may improve sample stability by reducing transphosphorylation. We found that extraction in the presence of 1% w/v (n-Dodecyl-β-D-maltoside) DDM worked best for yields and homogeneity, consistent with earlier studies that purified near full-length EGFR (Mi et al., 2008; Mi et al., 2011). Following solubilization in detergent micelles, excess cell debris were removed by centrifugation and the clarified lysate was subject to overnight Flag pulldown with Flag resin. The receptor-bound beads were washed in serial-batch mode in a buffer containing 0.5 mM DDM (2–3x critical micelle concentration, CMC) and eluted in 5 column volumes (CVs) of buffer with Flag peptide. Curiously, two other species were stoichiometrically co-enriched with near full-length HER3 after the one-step purification (see Fig. 2A). Eluate was then concentrated in 0.5 mL 100 kDa cutoff spin concentrators (Amicon) and injected over a Superose6 10/300 Increase column (GE Healthcare) pre-equilibrated in 0.5 mM DDM buffer. A representative gel filtration chromatogram is shown in Fig. 2B, blue curve). A step-by-step purification protocol is provided below.

Purification Protocol of Near Full-length HER3 in DDM—Buffers:

- **Lysis Buffer:** 50 mM TrisCl, 150 mM NaCl, 1 mM EDTA, pH 7.5 at 4°C, 1 mM $NaVO_3$, 1mM NaF, Roche Protease Inhibitor Tablet Cocktail - 1 pellet dissolved in 50 mL of buffer, DNase, and 1% w/v DDM (Inalco).
- **Flag Equilibration Buffer:** 50 mM TrisCl, 150 mM NaCl, pH 7.5 at 4°C, 0.5 mM DDM (Anatrace).
- **Flag Elution Buffer:** 50 mM TrisCl, 150 mM NaCl, pH 7.5 at 4 °C, 0.5 mM DDM (Anatrace), 250 mg/mL of Flag peptide (SinoBiological)
- **SEC Buffer:** same as Flag Equilibration Buffer

1. **Cell lysis.** Pellets stored in −80°C were thawed on ice for ~ 30 min. To soften the pellet, 10 mL of chilled lysis buffer was incubated with the pellet for an

additional 30 min. The pellet was gently resuspended in Lysis Buffer by gently pipetting with a 10 ml pipette until homogeneous and placed on a rotator for 1–2 hrs. Complete lysis was judged by the homogeneity of the resulting solution and the presence of DNA aggregate.

2. **Clarification.** Cells were spun down in 50 ml conical tubes at 4000xg for 20 min at 4°C in an Allegra X-15R (Beckman Coulter) refrigerated centrifuge to separate cell debris from detergent solubilized lysate.

3. **Equilibration of Flag Resin.** 2 mL of 50% resin slurry of Genscript G1 Flag resin was mixed with 8 mL of Flag Equilibration Buffer in a conical tube. The resin was gently pelleted at 500xg in an Allegra X-15R (Beckman Coulter) refrigerated centrifuge, for 2 min, 4°C and the residual Flag Equilibration Buffer was aspirated. The wash was repeated for a total of 3 serial washes in Flag Equilibration Buffer.

4. **Incubation with Flag Resin.** The clarified lysate was incubated with Flag Resin overnight at 4°C on a gently rocking platform.

5. **Flag Resin Wash.** The clarified lysate was separated from receptor-bound Flag Resin through gentle centrifugation at 500xg in an Allegra X-15R (Beckman Coulter) for 2 min, 4°C in conical tubes. The Flag Resin was then mixed in 10 column volumes (CVs) of Flag Equilibration Buffer and gently pelleted by centrifugation at 500xg in an Allegra X-15R. The washes were serially repeated for a total of 4 times.

6. **Flag Elution.** To elute the receptor from the resin, 3 CVs of Flag Elution Buffer was incubated with receptor-bound Flag Resin and incubated for 1 hr at 4°C on a rotating platform. The resin-eluate mixture was placed over a 1 mL gravity flow column to segregate resin from eluate. The residual Flag Resin was regenerated with serial gentle washes in 0.1M glacial acetic acid and 3x in water in the Allegra X-15R centrifuge (akin to serial washes in Step 5) for subsequent use.

7. **Concentration.** The eluted receptor was serially concentrated in 5 min increments with a 0.5 mL 100 kDa cutoff spin concentrators (Amicon) pre-equilibrated with Flag Equilibration Buffer at 3,000xg, 4°C to a final volume of 0.5 mL.

8. **Gel Filtration:** A Superose6 10/300 Increase (GE Healthcare) column was equilibrated with SEC buffer for two CVs using an Akta Pure chromatography instrument. The concentrated eluate was injected over the column at a flow rate of 0.5 mL/min at 4°C and 0.5 mL fractions were collected for further analysis.

The broader than expected peak on gel filtration is likely indicative of both receptor oligomeric and compositional heterogeneity. The two lower molecular weight bands are present in all fractions of the peak (data not shown). Mass spectrometry analysis identified band 1 in 2A as the chaperone heat shock protein 70 (Hsp70). Band 2 was not clearly identified by mass spectrometry. The tight association with chaperones may be an artifact of overexpression or could represent a physiologic association of the HER3 intracellular

domains with chaperones to regulate activity. Nevertheless, the sample heterogeneity poses a significant obstacle to structure determination.

We hypothesized that kinase domain stabilization with small molecule inhibitors may improve homogeneity. Bosutinib, a Src inhibitor, has been shown to bind and stabilize the HER3 kinase (Davis et al., 2011; Levinson & Boxer, 2014). A unique advantage of our expression system is that we may express our receptors in the presence of high affinity kinase inhibitors that would be cost inefficient at higher culture volumes. We therefore expressed near full-length HER3 with bosutinib (10 μM final concentration) added contemporaneously with the enhancers to the culture medium. We observed increased homogeneity after only one affinity purification step and a more monodisperse peak by gel filtration (Fig. 2B, pink curve). Our extrapolated final yield after purification was ~10 mg/L rendering only 30 mL of mammalian suspension culture sufficient for cryo-electron microscopy (Cryo-EM).

3.2 Characterization by Negative Stain Electron Microscopy

Diluted sample from the peak fraction of HER3 expressed with bosutinib was applied on carbon coated copper grids, stained with 0.75% uranyl formate, and imaged on an FEI-Tecnai T12 with a 4k CCD camera (Gatan). Negative stain micrographs were processed in Relion and resulting class averages revealed a “tri-lobular” shape (Fig. 3A). Only two of the lobes could be explained by a lateral projection of the previously published crystal structure of the HER3 unliganded extracellular domain (Cho & Leahy, 2002) (Fig. 3B). The third lobe may correspond to the micelle or a combination of the micelle and kinase.

3.3 Initial Attempts at Visualization by Single Particle Cryo-Electron Microscopy

Near full-length HER3 expressed with bosutinib was concentrated to 7.7 mg/mL (66 μM) and 3μL was applied onto negatively glow discharged Quantifoil R1.2/1.3 mesh Au holey-carbon grids under standard blotting conditions using a Vitrobot Mark IV (FEI) and plunge frozen in liquid ethane (negative glow discharge 30 sec, blot force 4, 100% humidity, 4°C, 6 seconds blot time). We found aggregated particles at 7.7 mg/mL (Fig. 3C) and no particles in the holes at lower concentrations (Fig. 3C). We hypothesized that the background DDM micelle may preferentially coat the air-water interface to prevent HER3 particles from entering thin ice and thus necessitating high receptor concentrations that promote sample aggregation.

4. The Detergent Exchange Strategy

4.1 Detergent Exchange into LMNG and visualization by Cryo-Electron Microscopy

We rationalized that either exchanging the detergent or eliminating the background detergent in the buffer would reduce the need to achieve high sample concentrations. We therefore selected a limited set of detergents to exchange the sample into based on chemical properties and previous success in high resolution membrane protein structural studies. We evaluated sample homogeneity through gel filtration and negative stain EM.

The ultra-low CMC detergent, LMNG, is structurally similar to DDM yet does not require background detergent to maintain the micelle (Stetsenko & Guskov, 2017). Glyco diosgenin (GDN) is structurally similar to digitonin and previous works on EGFR and HER2/HER3 heterodimer suggests that digitonin facilitates kinase stability (Choi et al., 2020; Mi et al., 2008). Like LMNG, the amphiphile 1,2,5,6-tetra-beta-D-glucopyranoside-3,4-O-Di-dodecyl-D-mannitol (MNA-C12) has an ultra-low CMC and has been successfully employed in structure determination (Benton et al., 2018).

We exchanged HER3 with bosutinib into 4 different conditions (0.01% w/v LMNG, 0.1% w/v LMNG, 0.06% w/v GDN, and 0.002% w/v MNA-C12) in a stepwise manner over the Flag wash step. Two concentrations of LMNG were chosen given that both were successfully applied in single particle cryo-EM. A detailed protocol is provided below:

Detergent Exchange Purification Protocol—Additional Buffers:

- **LMNG Wash Buffers:** 50 mM TrisCl, 150 mM NaCl, pH 7.5 at 4°C, 0.1% w/v (or 0.01% w/v) LMNG (Anatrace)
- **MNA-C12 Wash Buffer:** 50 mM TrisCl, 150 mM NaCl, pH 7.5 at 4°C, 0.002% w/v MNA-C12 (Anatrace)
- **GDN Wash Buffer Buffer:** 50 mM TrisCl, 150 mM NaCl, pH 7.5 at 4°C, 0.06% w/v GDN (Anatrace)
- **LMNG Flag Elution Buffer:** 50 mM TrisCl, 150 mM NaCl, pH 7.5 at 4°C, 0.1% w/v (or 0.01% w/v) LMNG (Anatrace), 250 mg/mL of Flag peptide (SinoBiological)
- **MNA-C12 Flag Elution Buffer:** 50 mM TrisCl, 150 mM NaCl, pH 7.5 at 4°C, 0.002% w/v MNA-C12 (Anatrace), 250 mg/mL of Flag peptide (SinoBiological)
- **GDN Flag Elution Buffer:** 50 mM TrisCl, 150 mM NaCl, pH 7.5 at 4°C, 0.06% w/v GDN (Anatrace), 250 mg/mL of Flag peptide (SinoBiological)
- **TBS:** 50 mM TrisCl, 150 mM NaCl, pH 7.5 at 4°C

Steps 1–4 the same as Purification Protocol for Near-Full Length HER3.

5. **Flag Resin Wash and Detergent Exchange**. The clarified lysate was separated from receptor-bound Flag Resin through gentle centrifugation at 500xg in an Allegra X-15R (Beckman Coulter) for 2 min, 4°C in conical tubes. The Flag Resin was then mixed with 10 CVs of Flag Equilibration Buffer containing DDM and gently pelleted by centrifugation (500xg, Allegra X-15R, 5 min, 4°C). 10 mL of a 50/50 v/v mixture of DDM containing Flag Equilibration Buffer and LMNG Wash Buffer was made. The same 50/50 v/v mixture was made for MNA-C12 and GDN samples. The receptor-bound resin was then incubated with this mixture for 5 min and the resin was gently pelleted by centrifugation as before. The supernatant was discarded and another 10 CVs of 100% LMNG/MNA-C12/GDN Wash Buffer were applied followed by

centrifugation (centrifuge settings same as first and second washes) to separate the supernatant from the resin. This was repeated once more in a 4th wash step.

6. **Flag Elution.** To elute the receptor from the resin, 3 CVs of LMNG/MNA-C12/GDN Flag Elution Buffer was incubated with receptor-bound Flag Resin and incubated for 1 hr at 4°C on a rotating platform. The resin-eluate mixture was placed over a 1 mL gravity flow column to segregate resin from eluate. The residual Flag Resin was regenerated for subsequent use.

7. **Concentration.** The eluted receptor was serially concentrated with a 0.5 mL 100 kDa cutoff spin concentrators (Amicon) pre-equilibrated with LMNG/MNA-C12/GDN Flag Wash Buffer at 3,000 g, 4°C to a final volume of 0.5 mL. In serial concentration, 0.5 mL is first applied to the filter device and centrifuged. Buffer passes through to the cellulose membrane to the filtrate collection tube while the concentrated protein resides in the filter device. Additional eluted receptor is applied to the filter device to 0.5 mL and subjected to an additional round centrifugation. This process is repeated until the entire eluted receptor volume in the filter device is 0.5 mL.

8. **Gel Filtration:** A Superose6 10/300 Increase (GE Healthcare) column was equilibrated using an Akta Pure chromatography instrument with TBS for two CVs for the LMNG samples. The MNA-C12 and GDN receptor samples were equilibrated in respective Wash Buffers. The concentrated eluate was injected over the column via the Akta Pure at a flow rate of 0.5 mL/min at 4°C and 0.5 mL fractions were collected for further analysis.

Interestingly, we found a striking difference in receptor stability between 0.1% LMNG and 0.01% LMNG conditions. Although both samples were run on gel filtration without any background detergent, the majority of the 0.01% LMNG sample precipitated during concentration and the peak elution volume resembles a species larger than that of DDM and 0.1% LMNG samples (Fig. 2C). The detergent in the 0.01% LMNG sample is perhaps not high enough to completely exchange with DDM, resulting in exposed unstable hydrophobic transmembrane domains. The 0.1% LMNG sample recapitulated the DDM sample in both the gel filtration profile and NS-EM (Fig. 3A, middle class averages). Although 0.06% GDN resulted in similar tri-lobular NS-EM class averages from sample eluting near 15 ml (Figure 2D and Figure 3A, bottom class averages), the presence of background detergent rendered this sample less promising for cryo-EM. Like 0.01% LMNG, 0.002% MNA-C12 did not stabilize the sample.

Fractions corresponding to the gel filtration elution peak of the 0.1% LMNG sample were pooled and concentrated to 3.5 mg/mL (30 μM) and applied as with the DDM samples onto Quantifoil grids. A range of concentrations were frozen with a lower bound of 0.11 mg/mL. Remarkably, we found adequate particle density without aggregation at 0.11 mg/mL (0.9 μM) (Fig. 3C).

5. Reconstructions of the Fully-Glycosylated HER3 Extracellular Domain

5.1 Data collection and processing

The grid was imaged on a 200-keV ThermoFisher Talos Arctica electron microscope with a K3 direct electron detector (Gatan) in super-resolution mode at a physical pixel size of 1.82Å/pix with a dose rate of ~10 e^- per pixel per second. Images were recorded with a 15 s exposure over 115 frames with a dose rate of 0.4 $e^-/Å^2$/frame. A total of 1411 micrographs were collected.

1411 micrographs were corrected for motion and radiation damage with MotionCor2 and the resulting sums were imported in CryoSPARC2. The dataset underwent micrograph curation with a final stack of 1119 micrographs. Micrograph Contrast Transfer Function (CTF) parameters were estimated with the patch CTF job in CryoSPARC2. Particles were picked initially using a Gaussian blob as a reference to minimize bias and the resulting picks were extracted with 2x Fourier cropping and subjected to iterative rounds of *ab initio* and heterogeneous refinements. The particles subclassified into two reconstructions representing two conformations (178,000 and 160,000 particles each) of the HER3 extracellular domain in solution (see section on Extracellular Dynamics). Collection and processing parameters are provided in Table 1.

5.2 Inconsistency between NS-EM and cryo-EM

Our extracellular domain cryo-EM reconstructions are consistent with the previously published model of the unliganded HER3 extracellular domain; domains I-IV of the extracellular module are resolved in the tethered, autoinhibited conformation. However, NS-EM class averages indicating a tri-lobular architecture are not recapitulated in 2D class averages or 3D volumes from cryo-EM (Fig. 4A). Two of the three lobes may be explained by bulky domains I and III of the HER3 extracellular domain. The third lobe, potentially micelle or kinase and micelle, is completely missing in cryo-EM. While it is plausible that unliganded HER3 may be highly dynamic, especially at the juxtamembrane segments, we would expect to see such dynamics in NS-EM processing. The fact that there is a discordance between NS-EM and cryo-EM with the same sample indicates that another phenomenon may account for the discrepancy, such as denaturation at the air-water interface. Recent studies with full-length Insulin Receptor (InsR), Insulin-like Growth Factor Receptor, and EGFR homodimers have also failed to reveal micelle or submicelle density (Huang et al., 2020; Li et al., 2019; Uchikawa et al., 2019). This phenomenon could explain why to date we do not have a high-resolution reconstruction of a full-length receptor kinase. Our recent work on the HER2/HER3/NRG1β heterocomplex with graphene oxide (GO) supported grids suggests that submicelle density may be recovered through particle recentering (see Trenker *et al.* in this issue). Further investigation in this area is warranted.

5.3 Identification of glycans

Docking the crystal structure into the ~6Å (gold-standard Fourier Shell Correlation (FSC) at 0.143 as estimated in CryoSPARC) reconstruction revealed additional density corresponding to glycosylation sites (Fig. 4B). The FSC is a statistics-based resolution measurement based on correlations between two independent half reconstructions vs resolution, with

the 0.143 value commonly accepted as the “resolution” of a map (Rosenthal & Henderson, 2003). We could identify density for the previously noted glycosylation sites in the crystal structure (N250, N353, N408, N414, N437, N469, N522, and N566). Even at these moderate resolutions, sufficient density was found extending beyond the first GlcNAc present in the crystal structure at several sites such as at N469 (Fig. 4B).

5.4 Extracellular Dynamics

Subsequent 3D classification revealed two conformational states of the HER3 ECD with roughly equal particle distribution. The two states differ by a subtle rigid-body rotation of domain I relative to III resulting in slight movements of the flexible domains II and IV (Fig. 4C). We used Rosetta flexible fitting protocol in torsion space to fit the crystal structure of unliganded HER3 extracellular domain (PDB ID: 1M6B) into each cryo-EM class and superimposed the resulting models(Wang et al., 2016). The movement of domain III relative to domain I is readily visualized through the models (Fig. 4D). The presence of multiple receptor conformations in solution is intriguing and may potentially resemble receptor states with different ligand affinities. These dynamics may provide an additional and previously unappreciated layer of receptor regulation.

6. Conclusion

Biophysical pursuits on full-length receptor kinases have been hampered by challenges in expression, purification, and visualization. Here, we demonstrate the markedly efficient expression of near full-length HER3 in Expi293 mammalian suspension cell culture such that only 30 mL are sufficient for cryo-EM. The efficiency enables small-scale parallelizability to accelerate optimization in sample homogeneity. Although this expression technique may not be generalizable to all receptor kinases, it provides a valuable starting point from which further modifications can be made. Similarly, our detergent exchange strategy from DDM to LMNG enables freezing at lower concentrations for cryo-EM which may be beneficial for samples prone to aggregation or receptors with inherently low yields. The ability to isolate near full-length HER3 enables future biophysical applications including the potential to reconstitute HER3 in lipid nanodiscs to probe receptor-membrane interactions or evaluate therapeutics in the near full-length context.

REFERENCES

Azimzadeh Irani M, Kannan S, & Verma C (2017, Aug). Role of N-glycosylation in EGFR ectodomain ligand binding. Proteins, 85(8), 1529–1549. 10.1002/prot.25314 [PubMed: 28486782]

Benton DJ, Nans A, Calder LJ, Turner J, Neu U, Lin YP, Ketelaars E, Kallewaard NL, Corti D, Lanzavecchia A, Gamblin SJ, Rosenthal PB, & Skehel JJ (2018, Oct 2). Influenza hemagglutinin membrane anchor. Proc Natl Acad Sci U S A, 115(40), 10112–10117. 10.1073/pnas.1810927115 [PubMed: 30224494]

Bouyain S, Longo PA, Li S, Ferguson KM, & Leahy DJ (2005, Oct 18). The extracellular region of ErbB4 adopts a tethered conformation in the absence of ligand. Proc Natl Acad Sci U S A, 102(42), 15024–15029. 10.1073/pnas.0507591102 [PubMed: 16203964]

Chen PH, Unger V, & He X (2015, Dec 4). Structure of Full-Length Human PDGFRbeta Bound to Its Activating Ligand PDGF-B as Determined by Negative-Stain Electron Microscopy. J Mol Biol, 427(24), 3921–3934. 10.1016/j.jmb.2015.10.003 [PubMed: 26463591]

Cho H-S, & Leahy DJ (2002). Structure of the Extracellular Region of HER3 Reveals an Interdomain Tether. Science, 297, 1330–1333. [PubMed: 12154198]

Choi B, Cha M, Eun GS, Lee DH, Lee S, Ehsan M, Chae PS, Heo WD, Park Y, & Yoon TY (2020, Apr 8). Single-molecule functional anatomy of endogenous HER2-HER3 heterodimers. Elife, 9. 10.7554/eLife.53934

Davis MI, Hunt JP, Herrgard S, Ciceri P, Wodicka LM, Pallares G, Hocker M, Treiber DK, & Zarrinkar PP (2011, Oct 30). Comprehensive analysis of kinase inhibitor selectivity. Nat Biotechnol, 29(11), 1046–1051. 10.1038/nbt.1990 [PubMed: 22037378]

Diwanji D, Thaker T, & Jura N (2019, Jun). More than the sum of the parts: Toward full-length receptor tyrosine kinase structures. IUBMB Life, 71(6), 706–720. 10.1002/iub.2060 [PubMed: 31046201]

Diwanji D, Trenker R, Thaker TM, Wang F, Agard DA, Verba KA, & Jura N (2021). Structures of the active HER2/HER3 receptor complex reveal dynamics at the dimerization interface induced by binding of a single ligand. bioRxiv. 10.1101/2021.05.03.442258

Du Z, & Lovly CM (2018, Feb 19). Mechanisms of receptor tyrosine kinase activation in cancer. Mol Cancer, 17(1), 58. 10.1186/s12943-018-0782-4 [PubMed: 29455648]

Ferguson K, Berger M, Mendrola J, Cho H-S, Leahy DJ, & Lemmon MA (2003). EGF Activates Its Receptor by Removing Interactions with Autoinhibit Ectodomain Dimerization. Molecular Cell, 11, 507–517. [PubMed: 12620237]

Goh LK, & Sorkin A (2013, May 1). Endocytosis of receptor tyrosine kinases. Cold Spring Harb Perspect Biol, 5(5), a017459. 10.1101/cshperspect.a017459 [PubMed: 23637288]

Gutmann T, Kim KH, Grzybek M, Walz T, & Coskun U (2018, May 7). Visualization of ligand-induced transmembrane signaling in the full-length human insulin receptor. J Cell Biol, 217(5), 1643–1649. 10.1083/jcb.201711047 [PubMed: 29453311]

Guy PM, Platko JV, Cantley L, Cerione RA, & Carraway KL (1994). Inset cell-expressed p180erbB3 possesses an impaired tyrosine kinase activity. Proc Natl Acad Sci U S A, 91, 8132–8136. [PubMed: 8058768]

Hellyer N, Cheng K, & Koland JG (1998). ErbB3 (HER3) Interaction with the p85 Regulatory Subunit of Phosphoinositide 3-kinase. Biochemical J, 333, 757–763.

Hsieh AC, & Moasser MM (2007, Aug 20). Targeting HER proteins in cancer therapy and the role of the non-target HER3. Br J Cancer, 97(4), 453–457. 10.1038/sj.bjc.6603910 [PubMed: 17667926]

Huang Y, Ognjenović J, Karandur D, Merk A, Subramaniam S, & Kuriyan J (2020). A structural mechanism for the generation of biased agonism in the epidermal growth factor receptor. bioRxiv. 10.1101/2020.12.08.417006

Jura N, Shan Y, Cao X, Shaw DE, & Kuriyan J (2009, Dec 22). Structural analysis of the catalytically inactive kinase domain of the human EGF receptor 3. Proc Natl Acad Sci U S A, 106(51), 21608–21613. 10.1073/pnas.0912101106 [PubMed: 20007378]

Kandoth C, McLellan MD, Vandin F, Ye K, Niu B, Lu C, Xie M, Zhang Q, McMichael JF, Wyczalkowski MA, Leiserson MDM, Miller CA, Welch JS, Walter MJ, Wendl MC, Ley TJ, Wilson RK, Raphael BJ, & Ding L (2013, Oct 17). Mutational landscape and significance across 12 major cancer types. Nature, 502(7471), 333–339. 10.1038/nature12634 [PubMed: 24132290]

Kovacs E, Zorn JA, Huang Y, Barros T, & Kuriyan J (2015). A structural perspective on the regulation of the epidermal growth factor receptor. Annu Rev Biochem, 84, 739–764. 10.1146/annurev-biochem-060614-034402 [PubMed: 25621509]

Lemmon MA, & Schlessinger J (2010, Jun 25). Cell signaling by receptor tyrosine kinases. Cell, 141(7), 1117–1134. 10.1016/j.cell.2010.06.011 [PubMed: 20602996]

Levinson NM, & Boxer SG (2014, Feb). A conserved water-mediated hydrogen bond network defines bosutinib's kinase selectivity. Nat Chem Biol, 10(2), 127–132. 10.1038/nchembio.1404 [PubMed: 24292070]

Li J, Choi E, Yu H, & Bai XC (2019, Oct 8). Structural basis of the activation of type 1 insulin-like growth factor receptor. Nat Commun, 10(1), 4567. 10.1038/s41467-019-12564-0 [PubMed: 31594955]

Lu C, Mi LZ, Grey MJ, Zhu J, Graef E, Yokoyama S, & Springer TA (2010, Nov). Structural evidence for loose linkage between ligand binding and kinase activation in the epidermal growth factor receptor. Mol Cell Biol, 30(22), 5432–5443. 10.1128/MCB.00742-10 [PubMed: 20837704]

Mi LZ, Grey MJ, Nishida N, Walz T, Lu C, & Springer TA (2008). Functional and Structural Stability of the Epidermal Growth Factor Receptor in Detergent Micelles and Phospholipid Nanodiscs. Biochemistry, 47, 10314–10323. [PubMed: 18771282]

Mi LZ, Lu C, Li Z, Nishida N, Walz T, & Springer TA (2011, Aug 7). Simultaneous visualization of the extracellular and cytoplasmic domains of the epidermal growth factor receptor. Nat Struct Mol Biol, 18(9), 984–989. 10.1038/nsmb.2092 [PubMed: 21822280]

Moasser MM (2007, Oct 4). The oncogene HER2: its signaling and transforming functions and its role in human cancer pathogenesis. Oncogene, 26(45), 6469–6487. 10.1038/sj.onc.1210477 [PubMed: 17471238]

Opatowsky Y, Lax I, Tome F, Bleichert F, Unger VM, & Schlessinger J (2014, Feb 4). Structure, domain organization, and different conformational states of stem cell factor-induced intact KIT dimers. Proc Natl Acad Sci U S A, 111(5), 1772–1777. 10.1073/pnas.1323254111 [PubMed: 24449920]

Peiris D, Spector AF, Lomax-Browne H, Azimi T, Ramesh B, Loizidou M, Welch H, & Dwek MV (2017, Feb 22). Cellular glycosylation affects Herceptin binding and sensitivity of breast cancer cells to doxorubicin and growth factors. Sci Rep, 7, 43006. 10.1038/srep43006 [PubMed: 28223691]

Rosenthal PB, & Henderson R (2003, Oct 31). Optimal determination of particle orientation, absolute hand, and contrast loss in single-particle electron cryomicroscopy. J Mol Biol, 333(4), 721–745. 10.1016/j.jmb.2003.07.013 [PubMed: 14568533]

Stetsenko A, & Guskov A (2017). An Overview of the Top Ten Detergents Used for Membrane Protein Crystallization. Crystals, 7(7). 10.3390/cryst7070197

Sung LY, Chen CL, Lin SY, Li KC, Yeh CL, Chen GY, Lin CY, & Hu YC (2014, Aug). Efficient gene delivery into cell lines and stem cells using baculovirus. Nat Protoc, 9(8), 1882–1899. 10.1038/nprot.2014.130 [PubMed: 25010908]

Takahashi M, Hasegawa Y, Ikeda Y, Wada Y, Tajiri M, Ariki S, Takamiya R, Nishitani C, Araki M, Yamaguchi Y, Taniguchi N, & Kuroki Y (2013, Nov 15). Suppression of heregulin beta signaling by the single N-glycan deletion mutant of soluble ErbB3 protein. J Biol Chem, 288(46), 32910–32921. 10.1074/jbc.M113.491902 [PubMed: 24097984]

Uchikawa E, Choi E, Shang G, Yu H, & Bai XC (2019, Aug 22). Activation mechanism of the insulin receptor revealed by cryo-EM structure of the fully liganded receptor-ligand complex. Elife, 8. 10.7554/eLife.48630

Wang RY, Song Y, Barad BA, Cheng Y, Fraser JS, & DiMaio F (2016, Sep 26). Automated structure refinement of macromolecular assemblies from cryo-EM maps using Rosetta. Elife, 5. 10.7554/eLife.17219

Yokoe S, Takahashi M, Asahi M, Lee SH, Li W, Osumi D, Miyoshi E, & Taniguchi N (2007, Mar 1). The Asn418-linked N-glycan of ErbB3 plays a crucial role in preventing spontaneous heterodimerization and tumor promotion. Cancer Res, 67(5), 1935–1942. 10.1158/0008-5472.CAN-06-3023 [PubMed: 17332320]

Zhang X, Gureasko J, Shen K, Cole PA, & Kuriyan J (2006, Jun 16). An allosteric mechanism for activation of the kinase domain of epidermal growth factor receptor. Cell, 125(6), 1137–1149. 10.1016/j.cell.2006.05.013 [PubMed: 16777603]

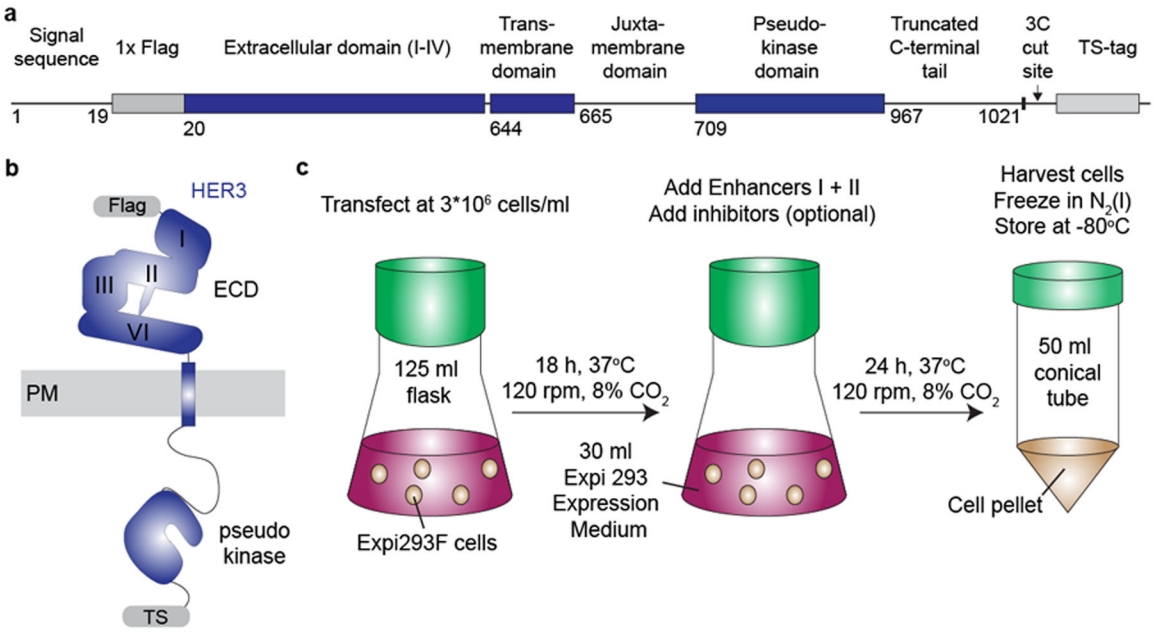

Figure 1. Construct Design and Mammalian Cell Expression of Near Full-Length HER3.

(A) Construct map of N-terminal Flag tagged HER3 (Δ1022-1342) with a C-terminal 3C protease site and twin-strep tag. (B) Cartoon of construct tagging scheme of near Full-Length HER3 comprising the extracellular, transmembrane, intracellular juxtamembrane, and pseudokinase domains. A 1x Flag tag precedes the N-terminus and the C-terminus is followed by a 3C protease cleavable twin-Strep tag. (C) Cartoon of expression method.

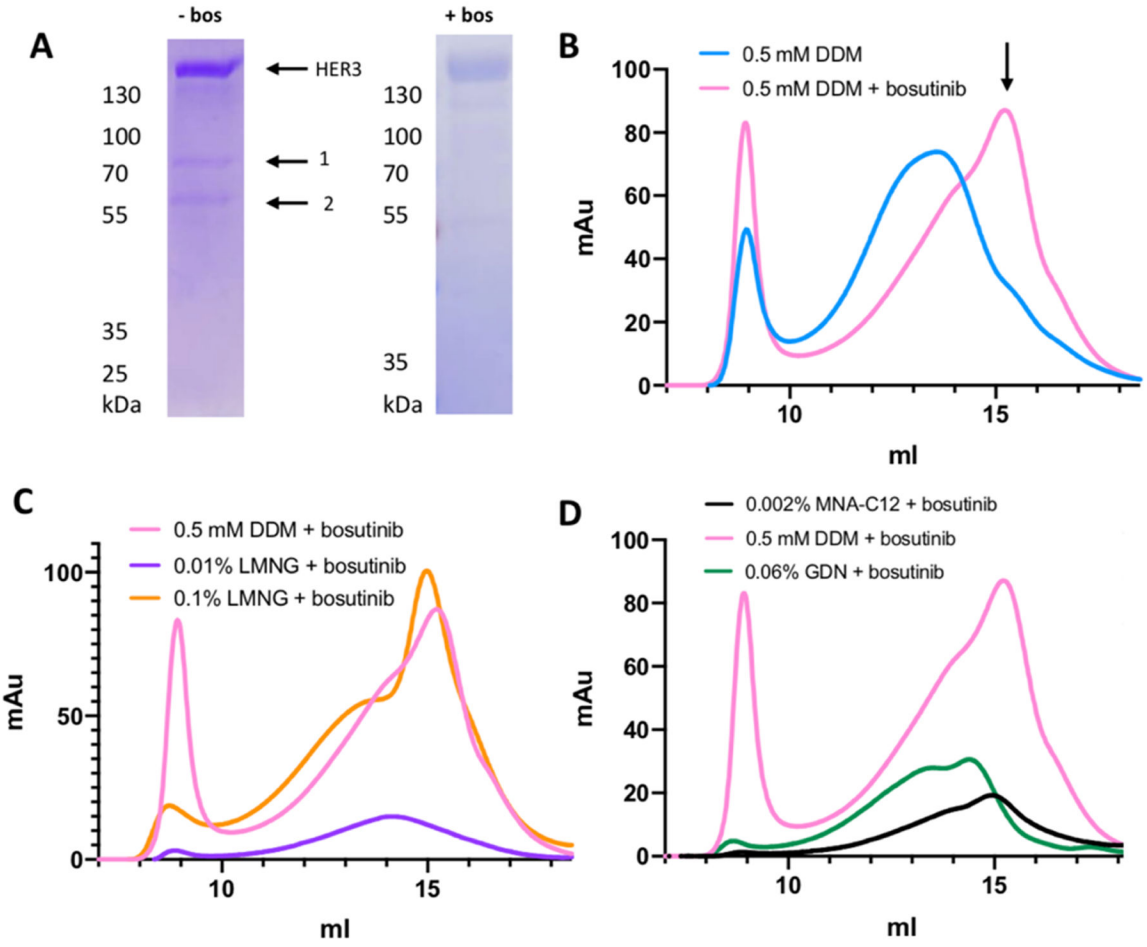

Figure 2. Purification of Near Full-Length HER3.

(A) Left, Flag eluate sample of near full-length HER3 in the absence of bosutinib (-bos) immunoprecipitated with two other bands (1 and 2). Right, the addition of bosutinib (+bos) during expression reduces the other two species. (B) Superimposed gel filtration chromatograms of near full-length HER3 on a Superose6 Increase 10/300 GL column in the presence and absence of bosutinib. Both samples were run in the presence of 0.5 mM DDM. (C) Superimposed gel filtration chromatograms of near full-length HER3 on a Superose6 Increase 10/300 GL column after exchange to 0.01% LMNG or 0.1% over Flag wash. Both LMNG samples were run on gel filtration in a buffer without detergent. The 0.5 mM DDM is the same as in (B). (D) Superimposed gel filtration chromatograms of near full-length HER3 on a Superose6 Increase 10/300 GL column after exchange to 0.002% MNA-C12 or 0.06% GDN over Flag wash.

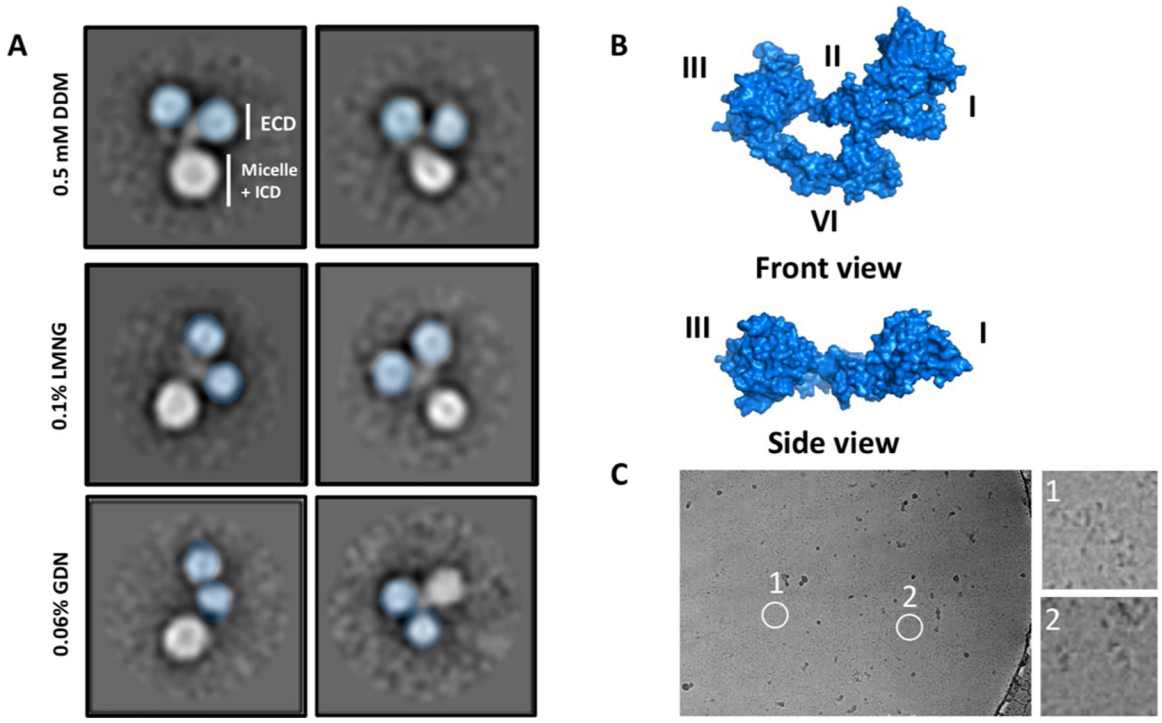

Figure 3. Negative Stain and Cryo-EM Freezing of Near Full-Length HER3.

(A) Top, representative NS-EM class averages of near full-length HER3 in the presence of 0.5 mM DDM. Middle, representative NS-EM class averages of near full-length HER3 in the presence of 0.1% LMNG. Bottom, representative NS-EM class averages of near full-length HER3 in the presence of 0.06% GDN. Density corresponding to putative extracellular domains I and III are colored in blue. (B) Surface cartoon of the HER3 extracellular domain crystal structure (PDB ID: 1M6B) viewed from the front and side. (C) Representative cryo-EM micrograph with particles more clearly visualized in the insets.

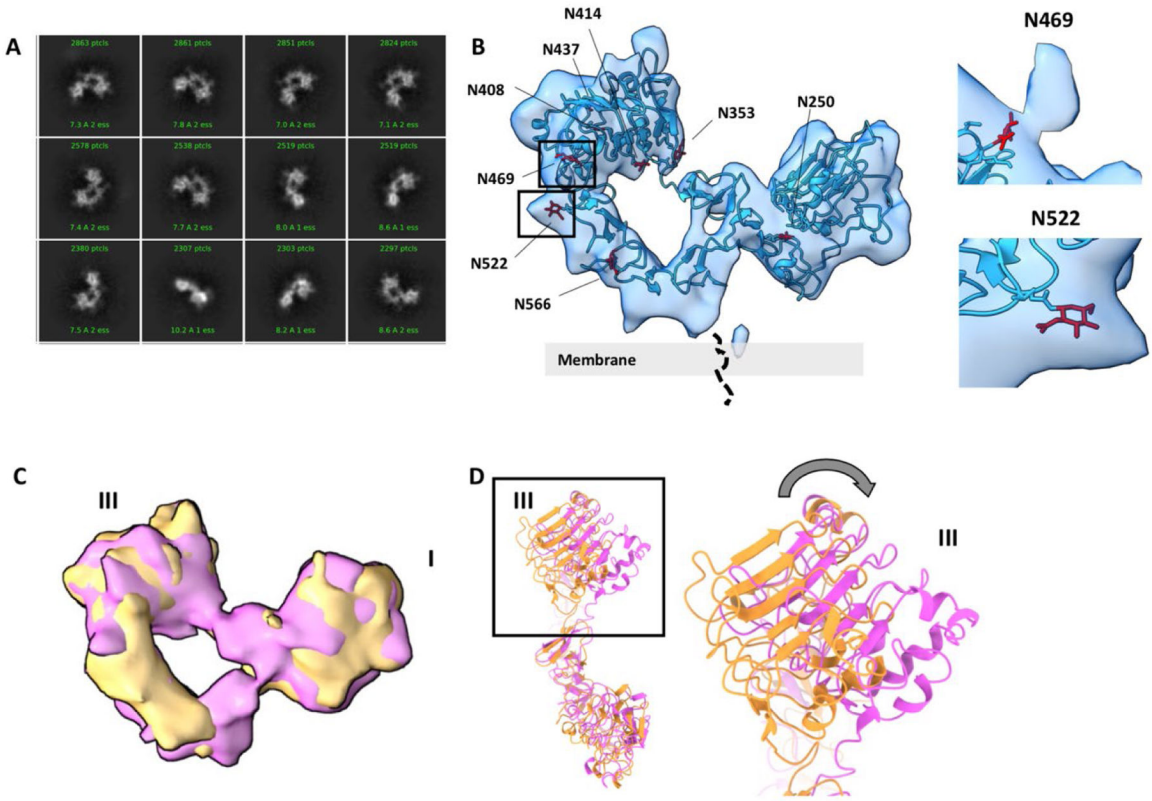

Figure 4. Reconstructions of the HER3 extracellular domain reveal glycosylation sites and dynamic properties.

(A) Representative cryo-EM 2D class averages of near full-length HER3 exchanged into 0.1% LMNG. (B) Rosetta fit model of the HER3 extracellular domain (PDB ID 1M6B) into the resulting cryo-EM reconstruction with N-linked glycans labeled. Insets highlight densities corresponding to N469 and N522. (C) Left, two resulting volumes after subclassification are superimposed. (D) Rosetta fit models for each volume overlayed to show movement of domain III relative to domain I in the inset.

Table 1:

Collection Statistics

	HER3 with Bosutinib
Data collection	
Microscope	Talos-Arctica
Voltage (keV)	200
Nominal Mag	22000x
Exposure navigation	Stage position/beam and image shift
Cumulative dose (e^{-}/Å^2)	46
Requested defocus range (um)	0.5–2.5
Detector	Gatan K3
Detector Operation Mode	CDS
Pixel size (physical pixel, Å)	1.82
Dose rate (e^{-}/physical pixel/sec)	10
Total exposure time (sec)	15.0
Exposure per frame (sec)	0.13
Micrographs collected	1411

Key Resources Tables

Chemicals, Resins, and Peptides	
REAGENT or RESOURCE	**SOURCE**
TRIS (Trizma Base)	Millipore Sigma, #T6066
NaCl	Millipore Sigma, #SX0420
Ethylenediaminetetraacetic acid (EDTA)	Millipore Sigma, #324503
Sodium orthovanadate ($NaVO_3$)	Millipore Sigma, #S6508
NaF	Millipore Sigma, # SX0550
cOmplete EDTA-free Protease Inhibitor Cocktail Mini Tablets	Roche, sold by Millipore Sigma, #11836170001
DNase I, grade II, from bovine pancreas	Roche, sold by Millipore Sigma, #10104159001
n-Dodecyl-β-D-Maltopyranoside (DDM), for gel filtration	Anatrace, #D310
n-Dodecyl-β-D-Maltopyranoside (DDM), for membrane extraction	Inalco, #1758–1350 Inalco brand was used to save costs during extraction
2,2-didecylpropane-1,3-bis-β-D-maltopyranoside (LMNG)	Anatrace, #NG310
DYKDDDDK synthetic peptide (Flag Peptide)	Sino Biological, #PP101274
Bosutinib (10mM in DMSO)	SelleckChem, #SKI-606
Anti-Flag resin (Anti-DYKDDDDK G1 Affinity Resin)	GenScript (#L00432-10)
Flag-HER3 (Δ1022-1342)-TS construct	In-house preparation
Uranyl formate	Electron Microscopy Sciences, #22450
GDN	Anatrace, #GDN101
MNA-C12	Anatrace, #MNA-C12
Cell Culture	
REAGENT or RESOURCE	**SOURCE**
Expi293	ThermoFisher Scientific
Expifectamine Kit	ThermoFisher Scientific
Expi293 Media	ThermoFisher Scientific
Software	
REAGENT or RESOURCE	**SOURCE**
PRISM	GraphPad
Rosetta	Downloaded from dimaiolab.ipd.uw.edu
CryoSPARC	Structura Biotechnology
Relion	Downloaded from www2.mrc-lmb.cam.ac.uk
MotionCor2	Downloaded from emcore.ucsf.edu
ChimeraX	Downloaded from rbvi.ucsf.edu